

## DEVELOPMENT AND DISEASE

# Impaired meiotic DNA-damage repair and lack of crossing-over during spermatogenesis in BRCA1 full-length isoform deficient mice

Xiaoling Xu<sup>1,2,\*</sup>, Olga Aprelikova<sup>3</sup>, Peter Moens<sup>4</sup>, Chu-Xia Deng<sup>2</sup> and Priscilla A. Furth<sup>1,5</sup>

<sup>1</sup>Department of Physiology, University of Maryland School of Medicine, Baltimore 21201, USA

<sup>2</sup>Genetics of Development and Disease Branch, 10/9N105, National Institute of Diabetes and Digestive and Kidney Diseases, National Institutes of Health, Bethesda, MD 20892, USA

<sup>3</sup>Laboratory of Biosystems and Cancer, 37/5016, Center for Cancer Research, National Cancer Institute, National Institutes of Health, Bethesda, MD 20892, USA

<sup>4</sup>Department of Biology, York University, Toronto, Ontario, M3J 1P3, Canada

<sup>5</sup>Department of Oncology, Lombardi Cancer Center, Georgetown University Medical Center, Washington, DC 20007, USA

\*Author for correspondence (e-mail: xiaolingx@intra.niddk.nih.gov)

Accepted 24 January 2003

## SUMMARY

Breast tumor suppressor gene 1 (*BRCA1*) plays an essential role in maintaining genomic integrity. Here we show that mouse *Brca1* is required for DNA-damage repair and crossing-over during spermatogenesis. Male *Brca1* <sup>$\Delta 11/\Delta 11$</sup> *p53*<sup>+/-</sup> mice that carried a homozygous deletion of *Brca1* exon 11 and a *p53* heterozygous mutation had significantly reduced testicular size and no spermatozoa in their seminiferous tubules. During spermatogenesis, homologous chromosomes from the mutant mice synapsed and advanced to the pachytene stage but failed to progress to the diplotene stage. Our analyses revealed that the *Brca1* mutation affected cellular localization of several DNA damage-repair proteins. This included prolonged association of  $\gamma$ H2AX with sites of DNA damage, reduced sex body formation, diminished Rad51 foci and absence

of Mlh1 foci in the pachytene stage. Consequently, chromosomes from mutant mice did not form chiasmata, a point that connects exchanging homologous chromosomes. *Brca1*-mutant spermatocytes also exhibited decreased RNA expression levels of several genes that are involved in DNA-damage repair, including RuvB-like DNA helicase, XPB, p62 and TFIID. Of note, the premature termination of spermatogenesis at the pachytene stage was accompanied by increased apoptosis by both p53-dependent and p53-independent mechanisms. Thus, our study revealed an essential role of *Brca1* in DNA-damage repair and crossing-over of homologous chromosomes during spermatogenesis.

Key words: BRCA1, MLH1,  $\gamma$ H2AX, Crossing-over, Apoptosis

## INTRODUCTION

Mammalian spermatogenesis proceeds through well-defined phases of mitotic and meiotic divisions as spermatogonia develop into spermatocytes, round spermatids and, finally, spermatozoa. In mice, all cell division in the testis is mitotic division before postnatal day 7 (P7). Starting from P8, spermatogonia enter the meiotic prophase of the meiotic pathway and homologous chromosomes undergo a programmed sequence of compaction, synapsis, recombination and segregation that leads to a reduction of genetic material from diploid to haploid (reviewed by Cohen and Pollard, 2001; Tarsounas and Moens, 2001; Zickler and Kleckner, 1999). A unique feature of meiosis I prophase chromatin is a high frequency of DNA double-strand breaks (DSBs), which are required for recombination between homologous chromosomes (reviewed by Cohen and Pollard, 2001; Roeder, 1997). Repair of DSBs is necessary to maintain genome

integrity and limit the mutational potential of these breaks. Loss-of-function mutations of many factors involved in DNA damage repair result in defective spermatogenesis (reviewed by Cohen and Pollard, 2001; Dasika et al., 1999; Tarsounas and Moens, 2001).

Germline mutations of *BRCA1* are found in approximately half of familial breast cancer cases and the majority of kindreds with combined familial breast and ovary cancer (Alberg and Helzlsouer, 1997; Brody and Biesecker, 1998; Paterson, 1998). *BRCA1* contains 24 exons that encode proteins of 1863 and 1812 amino acids in human and mouse, respectively (Lane et al., 1995; Miki et al., 1994). It has been shown that *BRCA1* contains multiple functional domains that interact with numerous molecules including products of tumor suppressor genes, oncogenes, DNA damage-repair proteins, cell-cycle regulators, ubiquitin hydrolases, and transcriptional activators and repressors (reviewed by Deng and Brodie, 2000). These observations indicate that *BRCA1* plays important roles in

multiple biological processes and pathways. Mutations of mouse *Brcal* using various gene-targeting constructs that introduce null, hypomorphic and tissue-specific mutations result in embryonic lethality, cellular growth defects, increased apoptosis, premature aging and/or tumorigenesis (Bachelier et al., 2003; Cao et al., 2003; Gowen et al., 1996; Hakem et al., 1996; Hohenstein et al., 2001; Liu et al., 1996; Ludwig et al., 1997; Ludwig et al., 2001; Shen et al., 1998; Xu et al., 1999a; Xu et al., 1999b; Xu et al., 2001).

Although pleiotropic effects are associated with *Brcal* mutations, it is generally believed that a major function of BRCA1 is to maintain genome integrity. For example, tumorigenesis following loss of BRCA1 function is a consequence of genome instability (Deng, 2001). *Brcal*-mutant embryos and embryonic fibroblast cells display hypersensitivity to  $\gamma$ -irradiation, demonstrating chromosome structural and numeric alterations, loss of G2/M cell-cycle checkpoint and centrosome amplification (Aprelikova et al., 2001; Shen et al., 1998; Xu et al., 1999a). Studies of somatic cell lines carrying mutations in either human *BRCA1* or mouse *Brcal* reveal essential functions of this gene in multiple DNA damage-repair pathways. This includes nuclear excision repair (Hartman and Ford, 2002), transcription-coupled repair of oxidative DNA damage (Abbott et al., 1999; Gowen et al., 1998), homologous recombinational repair (Moynahan et al., 1999; Moynahan et al., 2001; Snouwaert et al., 1999) and nonhomologous end-joining (Baldeyron et al., 2002; Zhong et al., 2002a; Zhong et al., 2002b). In conclusion, genetic instability associated with BRCA1 deficiency is caused, at least in part, by impaired DNA-damage repair.

Significantly, mice homozygous for a hypomorphic mutation of *Brcal* survive to adulthood in a *p53* (*Trp53* – Mouse Genome Informatics) null background at low frequency (Cressman et al., 1999). However, the two *Brcal* and *p53* double homozygous mutant (*Brcal*<sup>-/-</sup>*p53*<sup>-/-</sup>) male mice examined for this report were infertile because of azoospermia. Moreover, the number of apoptotic cells in the testes was increased, indicating that the germ cell death observed in *Brcal*<sup>-/-</sup>*p53*<sup>-/-</sup> mice was *p53*-independent. However, the reason why *Brcal* deficiency causes failure of spermatogenesis was not examined because of the difficulty in producing *Brcal*<sup>-/-</sup>*p53*<sup>-/-</sup> mice.

The *Brcal* gene is expressed in meiotic germ cells. Expression levels increase in the late pachytene and diplotene stages of meiosis I (Zabludoff et al., 1996). We hypothesized that the defect in spermatogenesis observed in *Brcal* mutant mice was secondary to inadequate DNA repair during meiosis. A mouse model that carried an in-frame deletion of *Brcal* exon 11 (*Brcal* <sup>$\Delta$ 11/ $\Delta$ 11</sup>) plus functional deletions of either one or both *p53* alleles was utilized to test this hypothesis. Although *Brcal* <sup>$\Delta$ 11/ $\Delta$ 11</sup> mice carrying two wild type *p53* alleles die in late gestation, they can survive to adulthood if one or both *p53* alleles (*Brcal* <sup>$\Delta$ 11/ $\Delta$ 11</sup>*p53*<sup>+/-</sup> or *Brcal* <sup>$\Delta$ 11/ $\Delta$ 11</sup>*p53*<sup>-/-</sup>) are mutated (Xu et al., 2001). In this study, these mice were used to demonstrate that deletion of *Brcal* exon 11 disrupts spermatogenesis but not oogenesis. Disruption of spermatogenesis was accompanied by both *p53*-independent and *p53*-dependent apoptosis, associated with altered RNA expression levels of a number of genes that are involved in DNA-damage repair and mislocalization of Rad51 and Mlh1.

These defects are accompanied by prolonged localization of  $\gamma$ H2AX, a DNA damage sensor, in nuclear foci, suggesting that the meiotic chromosomes from *Brcal* mutant mice accumulate unrepaired DNA damage.

## MATERIALS AND METHODS

### Testis preparation

*Brcal* <sup>$\Delta$ 11/ $\Delta$ 11</sup>*p53*<sup>+/+</sup>, *Brcal* <sup>$\Delta$ 11/ $\Delta$ 11</sup>*p53*<sup>+/-</sup>, *Brcal* <sup>$\Delta$ 11/ $\Delta$ 11</sup>*p53*<sup>-/-</sup> mice and control (*p53*<sup>+/+</sup>, *p53*<sup>+/-</sup> and *p53*<sup>-/-</sup>) mice were maintained in a mixed genetic background of 129/FVB/Black Swiss (Xu et al., 2001). BrdU was injected 2 hours prior to euthanasia. Testes were fixed in either Bouin's (for immunofluorescence studies) or 10% formalin (for BrdU labeling) for either 4 hours or overnight. Tissues were dehydrated in increasing ethanol concentrations (70%, 95%, 100%) for 30 minutes each. They then were treated 2 times with xylene (10 minutes each time), 1 time with a xylene/wax mixture at 50°C (1 hour), 3 times with wax alone (1 hour each time), followed by embedding in paraffin and sectioning at a thickness of 4-6  $\mu$ m. Sections either were stained with Hematoxylin and Eosin (H&E) or processed for immunohistochemical analysis using antibodies to germ cell nuclear antigen (GCNA) (1:50, a kind gift from Dr George Enders, University of Kansas Medical Center) or to antiphospho-histone H3 (Upstate, Biotechnology, Lake Placid, NY). Slides were examined and photographed under a light microscope.

### Preparation of chromosome spreads for immunofluorescence

Chromosome spreads were prepared from testes of P10-28 males and ovaries of embryonic day (E) 16.5-17.5 female embryos as described (Romanienko and Camerini-Otero, 2000). The slides bearing chromosome spreads were either used fresh or within two months of freezing at -20°C (slides thawed at room temperature for ~5 minutes). After washing with phosphate-buffered saline (PBS) three times for 5 minutes each, slides were processed for immunofluorescent staining using standard procedures. The first antibodies used were: RAD51 (SC-8349, Santa Cruz Biotechnology, Inc. Santa Cruz, CA at 1:100 dilution), DMC1 (SC-8973, Santa Cruz Biotechnology at 1:100 dilution), MLH1 (a mouse monoclonal antibody from Pharmingen, San Diego, CA at 1:100 dilution), rabbit anti-phospho-histone H2AX (a mouse monoclonal antibody from Upstate Biotechnology, Lake Placid, NY at 1:500 dilution) and rabbit anti-SCP3 antibody (Dobson et al., 1994). Alex-red 560 and green 488-conjugated secondary antibodies (Molecular Probes, Eugene, OR) were used at 1:500 dilution.

### Western blotting

Western blots were carried out using standard procedures using the following antibodies: goat anti-DMC1 at 1:1000 dilution (Santa Cruz Biotechnology); rabbit anti-RAD51 at 1:1000 dilution (Santa Cruz Biotechnology); mouse anti-MLH1 at 1:1000 dilution; and mouse anti-Pms2 at 1:1000 dilution (Pharmingen, San Diego, CA).

### Semiquantitative RT-PCR

Total RNA was extracted from testes at different developmental stages, including P14, P16, P21 and P22. Reverse-transcription reactions were carried out using a 1st strand cDNA-synthesis kit (Roche, Indianapolis, IN). The cDNA samples were stored at -20°C. One  $\mu$ g of RNA from each sample was used as template for each reaction and 1  $\mu$ l of cDNA from each sample was used for PCR reaction. The optimal number of cycles for amplification was determined according to the cycle number that yielded the strongest band in the linear range. The ranges of cycles varied from 25-28,



depending on the specific RNA target and primer set. The samples were heated to 94°C for 2 minutes and then run through 25–28 cycles of 94°C for 30 s, 60°C for 30 s and 72°C for 1 minute, followed by 72°C for 10 minutes and then 4°C. Primers used in this study and the DNA lengths amplified are shown below.

TFIIH amplification (680 bp):

5'-cagaaaatcagtcagaggg-3', 5'-ccctcgtctaaggttattc-3'

TFIID amplification (360bp):

5'-gttgaaacagacatggtttgc-3', 5'-cagccatgctaagaagctac-3'

RuvB amplification (540 bp):

5'-gacacaccattcacagccatc-3', 5'-gatctgttctcggacttctg-3'

GAPDH amplification (300 bp):

5'-acagccgcatcttctgtgc-3', 5'-ttgatgttagagggtctgc-3'

### TUNEL assay and BrdU-incorporation assay

Testis sections were analyzed for apoptosis using the ApoTag kit as recommended by the manufacturer (Intergen Company, Purchase, NY). To evaluate cellular proliferation rates, BrdU incorporation was measured using a cellular proliferation kit following the manufacturer's directions (Amersham Bioscience, England).

### $\gamma$ -Irradiation

Mice at 1 month of age were irradiated at 80 Gy (1Gy minutes<sup>-1</sup>, Gammacell 40) and were euthanized 10 minutes, 30 minutes, 2 hours and 4 hours after irradiation. Testes were removed and processed for chromosome spreads and immunofluorescence staining as described above.

### Statistical analyses

Student's *T* test was used to compare differences of pachytene and diplotene spermatocytes, rates of apoptosis, numbers of foci for Mlh1 and Rad51, and numbers of sex bodies for  $\gamma$ H2AX between *Brca1* mutant and control mice at ages specified in the text.  $P \leq 0.05$  was considered statistically significant.

## RESULTS

### Spermatogenesis is defective in *Brca1* <sup>$\Delta 11/\Delta 11$</sup> *p53*<sup>+/-</sup> male mice

Mature ( $\geq 6$  weeks of age) *Brca1* <sup>$\Delta 11/\Delta 11$</sup> *p53*<sup>+/-</sup> male mice ( $n=10$ ) contained no spermatozoa in their testes (Fig. 1B, and data not shown). To identify the earliest stages at which defective spermatogenesis occurred, testes from P10–28 *Brca1* <sup>$\Delta 11/\Delta 11$</sup> *p53*<sup>+/-</sup> mutant and *p53*<sup>+/-</sup> control mice were isolated and compared. At P10, testes of both *Brca1* mutant and control mice were similar in size (Fig. 1C). Histological analyses demonstrated no obvious differences in seminiferous tubule size and the numbers of spermatogonial cells (Fig. 1D,E). However, starting from P16, testes from *Brca1* <sup>$\Delta 11/\Delta 11$</sup> *p53*<sup>+/-</sup> mutant mice were significantly smaller than controls (Fig. 1F,I,L). In control mice, spermatocytes began to enter the diplotene stage at P16 and spermatocyte size increased (arrow, Fig. 1G), but no diplotene spermatocytes were detected in the testes from *Brca1* mutant mice (Fig. 1H). At P21, spermatocytes from control mice had finished meiosis and formed spermatids (arrow, Fig. 1J). No spermatids were found in the testes from *Brca1* mutant mice (Fig. 1K), instead, cells with dark

Hematoxylin-stained nuclei were found (arrow, Fig. 1K). This phenotype was apparent in the testes of *Brca1* mutant males from P28 to P90 (Fig. 1B,N and data not shown). These results indicate that spermatogenesis, including the first wave of spermatogenesis, did not progress beyond meiosis I in the *Brca1* mutant mice.

### Spermatogenesis is terminated prior to the diplotene stage of meiosis I in *Brca1* mutant males

Molecular markers were used to define the stages of meiosis I that were defective in the *Brca1* mutant male mice. GCNA is expressed specifically in premeiotic cells up to the pachytene

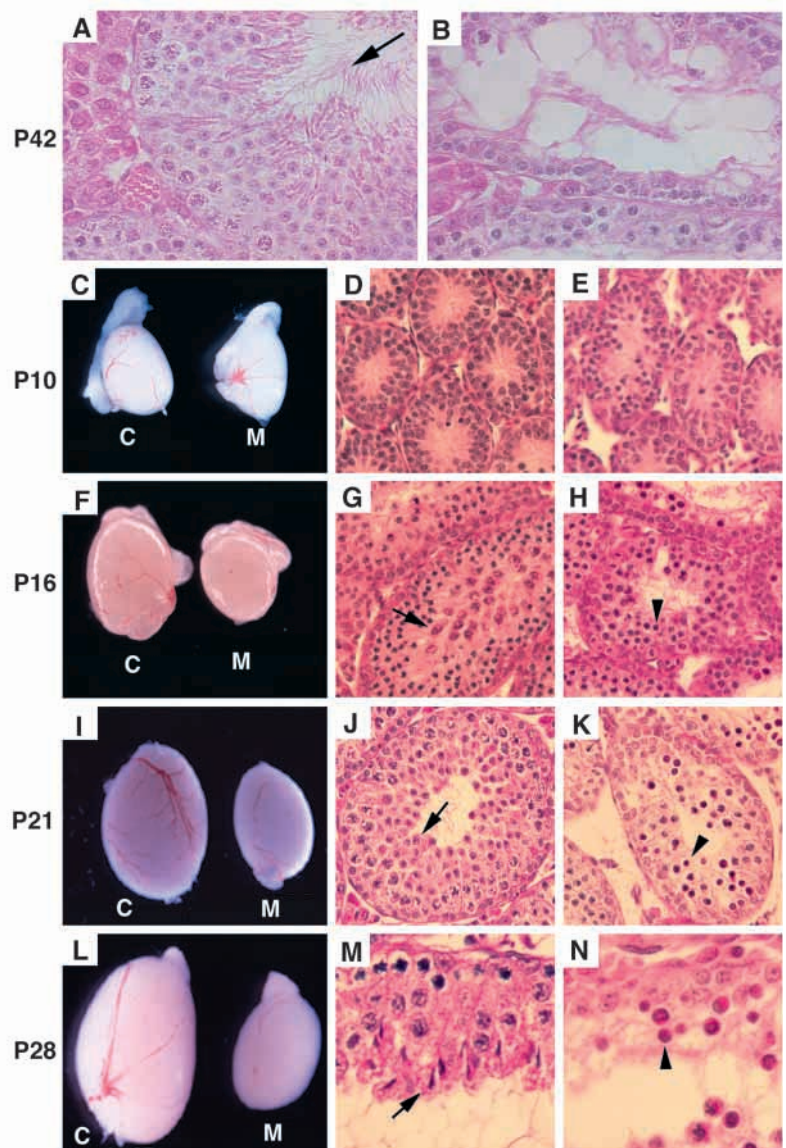


**Fig. 1.** Size and histology of testes from *p53*<sup>+/-</sup> control (C) and *Brca1* <sup>$\Delta$</sup> *p53*<sup>+/-</sup> mutant (M) mice. Ages of mice are indicated. (A,D,G,J,M) Control mice; (B,E,H,K,N) *Brca1* mutant mice. No significant difference in size was detected between control and mutant testes at postnatal day 10 (P10); however, mutant testes are smaller at P16 and older. Arrows indicate spermatozoa (A), diplotene spermatocytes (G), round spermatocytes (J) and differentiated spermatids (M). Mutant testes lack these cells. Arrowheads in H,K,N indicate condensed nuclei, which are TUNEL positive (see Fig. 3).



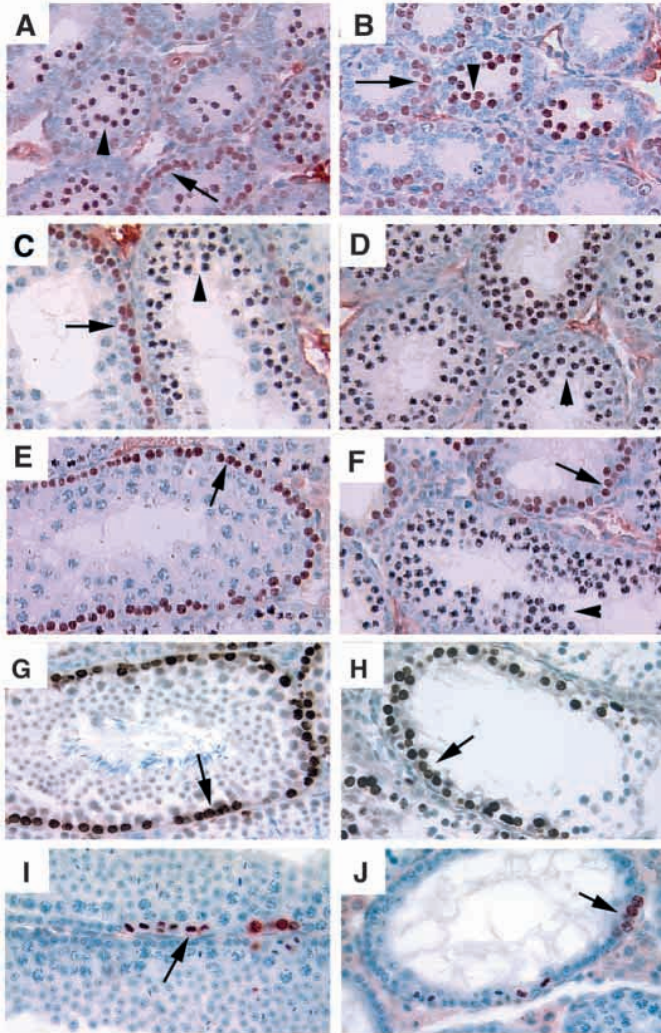


**Fig. 2.** Loss of the full-length isoform of *Brcal* does not interfere with the mitotic phase of spermatogenesis. Immunolocalization of GCNA in *p53*<sup>+/-</sup> control (A,C,E) and *Brcal*<sup>Δ/Δ</sup>*p53*<sup>+/-</sup> mutant (B,D,F) testes at P10 (A,B), P16 (C,D) and P21 (E,F). In control testes, early pachytene spermatocytes located inside the lumen (arrows) and premeiotic cells located along the base of tubules (arrowheads) are GCNA positive. By contrast, spermatocytes inside the lumen of *Brcal* mutant testes are all positive for GCNA (arrows and arrowheads, B,D,F). Anti-BrdU (G,H), and anti-phosphorylated H3 (I,J) staining in testes from 6-week-old control (G,I) and mutant (H,J) mice. Arrows in G-J indicate BrdU-positive cells (G,H) and phosphorylated H3-positive cells (I,J).

stage of meiosis I (Enders and May, 1994). The protein is degraded and no longer detected after the pachytene stage. At P10, the pattern of GCNA staining was similar in *Brcal* mutants and control mice (Fig. 2A,B). At P16, some GCNA-negative spermatocytes were found in the testes from control mice, whereas others still stained for GCNA (Fig. 2C). The change in the staining pattern indicated that some, but not all, spermatocytes had passed through the pachytene stage. By contrast, all spermatocytes from *Brcal* mutant males demonstrated GCNA staining at day P16 (Fig. 2D). At P21, only one layer of GCNA-positive spermatogonia was observed

on the tubular basement membrane in control mice, the majority of cells were GCNA negative (Fig. 2E). By contrast, all cells remained GCNA positive in *Brcal* mutant mice at P21 (Fig. 1F). The differences in staining patterns between the control and *Brcal* mutant mice indicated that spermatogenesis in *Brcal* mutant mice did not pass through the pachytene stage of meiosis I.

To determine if mitotic division in the testes was affected by mutation of *Brcal*, BrdU-labeling experiments were performed to identify rapidly dividing spermatogonial cells. No significant differences in rates of DNA synthesis between *Brcal* mutant and control mice were found (Fig. 2G,H). Similarly, there were no apparent differences in the staining patterns of an antibody to phosphorylated histone H3, which binds specifically to the chromatin of cells in the M phase of mitotic division (Chadée et al., 1995) (Fig. 2I,J). These experiments demonstrated that mitotic division was not impaired in the testes of *Brcal* mutant mice.

### Testes of *Brcal* mutant mice exhibit increased rates of apoptosis

The presence of prominent dark Hematoxylin-stained spermatocyte nuclei in the testes of *Brcal* mutant mice (Fig. 1K) suggested that the *Brcal* mutation caused increased rates of spermatocyte apoptosis. Tissue sections from testes of *Brcal*<sup>Δ11/Δ11</sup>*p53*<sup>+/-</sup> and *p53*<sup>+/-</sup> control mice at P10, P16 and P21 were analyzed by TUNEL assay to quantify these differences. At P10, <2% of seminiferous tubules in control and mutant testes contained apoptotic cells. This did not change in testes from control mice at P16 and P21. However, in *Brcal* mutant mice the number of seminiferous tubules that contained apoptotic spermatocytes increased significantly at P16 and P21 (22% and 30%, respectively) (Fig. 3A). To directly compare rates of cellular apoptosis, the percentage of apoptotic cells were determined in TUNEL-positive seminiferous tubules that were selected randomly from testes of ten control and ten *Brcal* mutant mice. At P10, in testes from both control and *Brcal* mutant mice fewer than 4% of cells were apoptotic (Fig. 3B). At P16 and P21 the percentage of apoptotic cells did not change in testes from control mice, but increased significantly to 40% at P16 and 50% at P21 (both  $P \leq 0.0001$  compared to control mice) in testes from *Brcal* mutant mice (Fig. 3B). Thus, the premature termination of spermatogenesis at the pachytene stage of meiosis I in *Brcal* mutant mice was accompanied by significantly increased rates of apoptosis.

Because activation of p53 induces apoptosis in a number of tissue/organ systems in *Brcal*<sup>Δ11/Δ11</sup> mutant mice (Xu et al., 1999b; Xu et al., 2001), we next determined whether the increased rate of apoptosis in the *Brcal* mutant testes was p53 dependent. Because only a few (1-2%) of *Brcal*<sup>Δ11/Δ11</sup>*p53*<sup>+/+</sup> male mice survive to adulthood (Xu et al., 2001), rates of apoptosis were compared in testes isolated from *Brcal*<sup>Δ11/Δ11</sup>*p53*<sup>+/+</sup>, *Brcal*<sup>Δ11/Δ11</sup>*p53*<sup>+/-</sup> and *Brcal*<sup>Δ11/Δ11</sup>*p53*<sup>-/-</sup> mice. TUNEL-positive cells were detected in testes of all three genotypes, indicating that the loss of p53 did not prevent apoptosis. In testes isolated from *Brcal*<sup>Δ11/Δ11</sup>*p53*<sup>+/+</sup> mice at P19 (Fig. 3C,D), the absolute numbers of apoptotic cells in each tubule was less than those found in testes from *Brcal*<sup>Δ11/Δ11</sup>*p53*<sup>+/-</sup> and *Brcal*<sup>Δ11/Δ11</sup>*p53*<sup>-/-</sup> mice. However, all

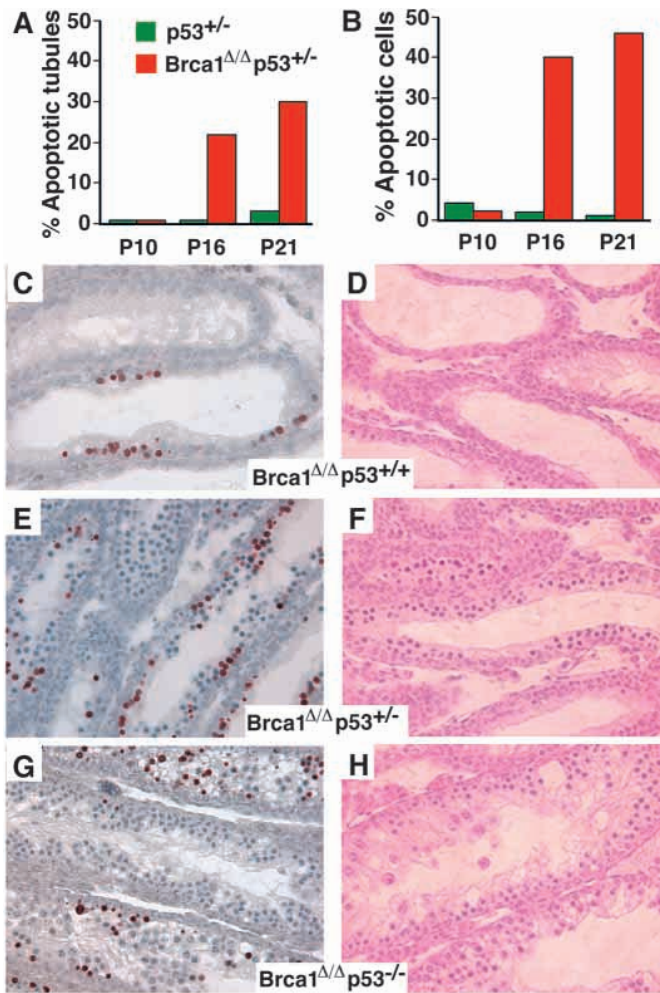


**Fig. 3.** Absence of the *Brca1* full-length isoform results in *p53*-dependent and *p53*-independent apoptosis. Percentages of seminiferous tubules containing TUNEL-positive cells (A) and percentages of TUNEL-positive cells (B) at P10, P16 and P21 in *p53*<sup>+/-</sup> and *Brca1*<sup>Δ/Δ</sup>*p53*<sup>+/-</sup> testes. TUNEL-positive cells in *Brca1*<sup>Δ/Δ</sup>*p53*<sup>+/+</sup> (P19) (C), *Brca1*<sup>Δ/Δ</sup>*p53*<sup>+/-</sup> (P21) (E) and *Brca1*<sup>Δ/Δ</sup>*p53*<sup>-/-</sup> (P21) (G) testes. Corresponding H&E-stained histological images are shown in D,F,H.

the tubules were nearly empty, suggesting either that more extensive cell death happened earlier in spermatogenesis or that germ cells did not robustly colonize the gonads during early development. A direct comparison between *Brca1*<sup>Δ/Δ</sup>*p53*<sup>+/-</sup> (Fig. 3E,F) and *Brca1*<sup>Δ/Δ</sup>*p53*<sup>-/-</sup> (Fig. 3G,H) testes demonstrated significant lower rates of apoptosis in *p53*<sup>-/-</sup> mice than in *p53*<sup>+/-</sup> mice. In ten, randomly selected TUNEL-positive seminiferous tubules from *Brca1*<sup>Δ/Δ</sup>*p53*<sup>-/-</sup> mice, 12% of cells were apoptotic at P16 and 22% at P21 compared to 40% at P16 and 50% at P21 in *Brca1*<sup>Δ/Δ</sup>*p53*<sup>+/-</sup> testes (Fig. 3B). Histological sections demonstrated a graded increase in the total number of spermatocytes when the number of wild type *p53* alleles decreased from 2 (*p53*<sup>+/+</sup>) to 0 (*p53*<sup>-/-</sup>) that correlated with the decreased number of apoptotic cells in testes isolated from *Brca1*<sup>Δ/Δ</sup>*p53*<sup>+/+</sup>, *Brca1*<sup>Δ/Δ</sup>*p53*<sup>+/-</sup> and *Brca1*<sup>Δ/Δ</sup>*p53*<sup>-/-</sup> mice. These results indicated that *Brca1* mutation triggered

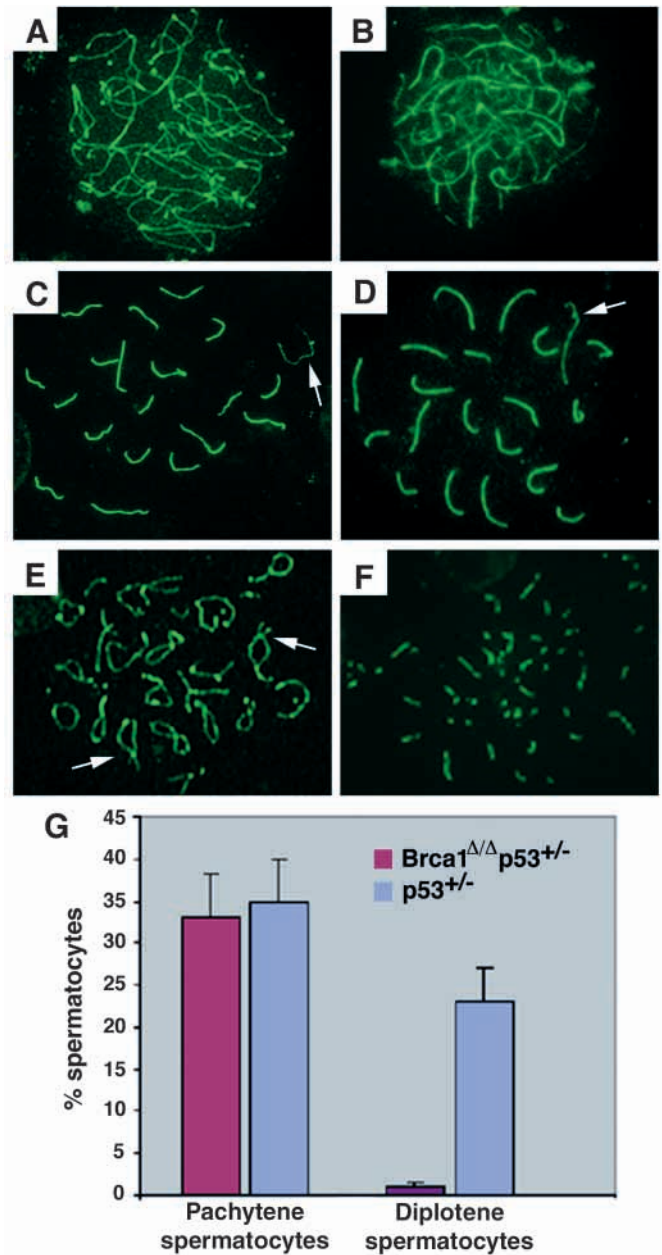


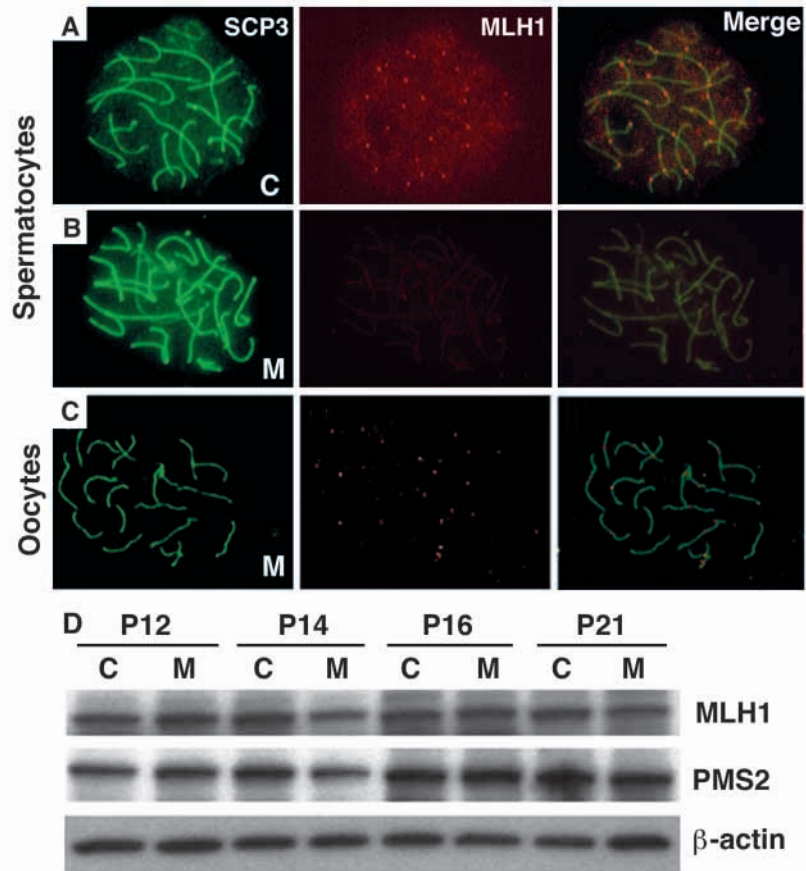
**Fig. 4.** Scp3 immunofluorescence staining of primary spermatocyte chromosomes from *p53*<sup>+/-</sup> control (A,C,E) and *Brca1*<sup>Δ/Δ</sup>*p53*<sup>+/-</sup> mutant (B,D,F) mice. (A,B) Zygotene, (C,D) pachytene and (E,F) diplotene spermatocytes. Arrows in C,D indicate paired XY chromosomes. Arrows in E indicate chiasmata in diplotene spermatocytes of control mice. No normal diplotene chromosome spreads were found in mutant spermatocytes, although some cells show fragmented cores/SCs (F). (G) Comparison of pachytene and diplotene stage spermatocytes at P16 and P21. Two-thousand meiosis I spermatocytes were counted. Data are plotted as average percentage (mean±s.d.) determined from four pairs of mutant and control mice. There were no statistically significant differences in the numbers of pachytene stage spermatocytes between mutant and control mice (synapses;  $P \geq 0.08$ ). A significant difference in the numbers of diplotene stage spermatocytes was observed (cross-over;  $P \geq 0.002$ ).

apoptosis through *p53*-dependent and *p53*-independent mechanisms.



**Fig. 5.** Localization of Mlh1 in *Brca1* mutant mice.

(A,B) Scp3 and Mlh1 double immunofluorescence staining of chromosomes prepared from  $p53^{+/-}$  control (A) and *Brca1* <sup>$\Delta11/\Delta11$</sup>  $p53^{+/-}$  mutant (B) spermatocytes at the pachytene stage. Three pairs of mutant and control mice at P16, P18 and P21 were examined. There were no significant differences in Mlh1 foci formation between *Brca1* mutant and control mice in ( $P \leq 0.0001$ ). (C) Scp3 and Mlh1 double immunofluorescence localization of chromosomes prepared from *Brca1* <sup>$\Delta11/\Delta11$</sup>  $p53^{+/-}$  oocytes. More than 10 mutant and control embryos at E16.5-17.5 were examined and no obvious differences were found. (D) Western blot analysis of Mlh1 and Pms2 in  $p53^{+/-}$  (C) and *Brca1* <sup>$\Delta11/\Delta11$</sup>  $p53^{+/-}$  (M) testes. Genotypes, ages and antibodies are indicated.



### The majority of homologous chromosomes from the testes of *Brca1* mutant mice are able to synapse but do not form crossing-overs

To determine whether or not the homologous synapsis process was impaired by *Brca1* mutation, testicular chromosome spreads were stained with an antibody to synaptonemal complex protein 3 (SCP3). SCP3 is one of the components of the axial and lateral element of the synaptonemal complex. It appears in leptotene stage spermatocytes and disappears in late meiotic cells (Dobson et al., 1994). Analysis of >2000 spermatocytes from *Brca1* <sup>$\Delta11/\Delta11$</sup>  $p53^{+/-}$  and control mice at P10-P21 demonstrated that the chromosomes from spermatocytes of *Brca1* mutant mice behaved normally until the pachytene stage (Fig. 4A-D). Only 3% of the cells showed delayed pairing of one or two chromosomes in *Brca1* mutant mice (data not shown). Chromosomal spreads prepared from P16 *Brca1* mutant and control mice demonstrated that approximately one third of spermatocytes in both strains completed synapses of homologous chromosomes (Fig. 4G). These observations were consistent with our earlier histological findings demonstrating that mutant spermatocytes developed relatively normally until the pachytene stage.

During normal spermatogenesis, diplotene stage spermatocytes begin to appear at P16 and represent 20-25% of the total spermatocyte population at P21 (Fig. 4E). A hallmark of chromosome behavior at these stages is the extensive separation of homologous chromosomes except for the crossing-over sites that are held by chiasmata (arrows, Fig. 4E). By contrast, few homologous chromosomes demonstrated separation in the spermatocytes from *Brca1* mutant mice and those few spermatocytes that were not already eliminated through apoptosis showed fragmented cores/synaptonemal complexes (Fig. 4F). In fact, <1% of spermatocytes from *Brca1* mutant mice exhibited even partial separation of their chromosomes (Fig. 4G). These observations demonstrated that spermatocytes from *Brca1* mutant mice were arrested at the late pachytene stage and failed to enter the diplotene stage.

### Absence of the *Brca1* full-length isoform diminishes Mlh1 foci on chromosomes

Many DNA damage-repair proteins, including MLH1, RAD51

and DMC1, are involved in the crossing-over process. To investigate the molecular mechanisms underlying the failure of crossing-over formation in spermatocytes from *Brca1* mutant mice, the expression patterns and sites of cellular localization of Mlh1, Rad51 and Dmc1 were determined.

In control mice, Mlh1 first appeared as distinct spots along the chromosomes of late zygotene spermatocytes and was maintained until the mid-pachytene stage in spermatocytes (Fig. 5A,  $n=267$ ). By contrast, no Mlh1 foci were observed on the majority (156 out of 162) of chromosome spreads prepared from late zygotene to mid-pachytene stage spermatocytes of *Brca1* mutant mice. The remaining six spermatocytes showed very weak staining (Fig. 5B). Western blotting was performed to determine whether the abnormal distribution of Mlh1 on the chromosomes from *Brca1* mutant mice was due to reduced protein concentrations of either Mlh1 or its binding partner Pms2. There were no obvious differences in the concentrations of these proteins between *Brca1* mutant and control mice at any of the stages examined (Fig. 5D). In conclusion, although the distribution of Mlh1 on chromosomes was abnormal in *Brca1* mutant mice, overall expression levels were normal. Because *Brca1* mutant females were fertile, localization of Mlh1 was also checked in female mice. Nearly all of the chromosomes isolated from 200 late zygotene to mid-pachytene stage oocytes taken from E16.5-17.5 *Brca1* <sup>$\Delta11/\Delta11$</sup>  $p53^{+/-}$  female embryos had Mlh1 foci. There were no obvious differences in either the localization pattern or intensity of the foci between *Brca1* mutant (Fig. 5C) and control (not shown) oocytes.

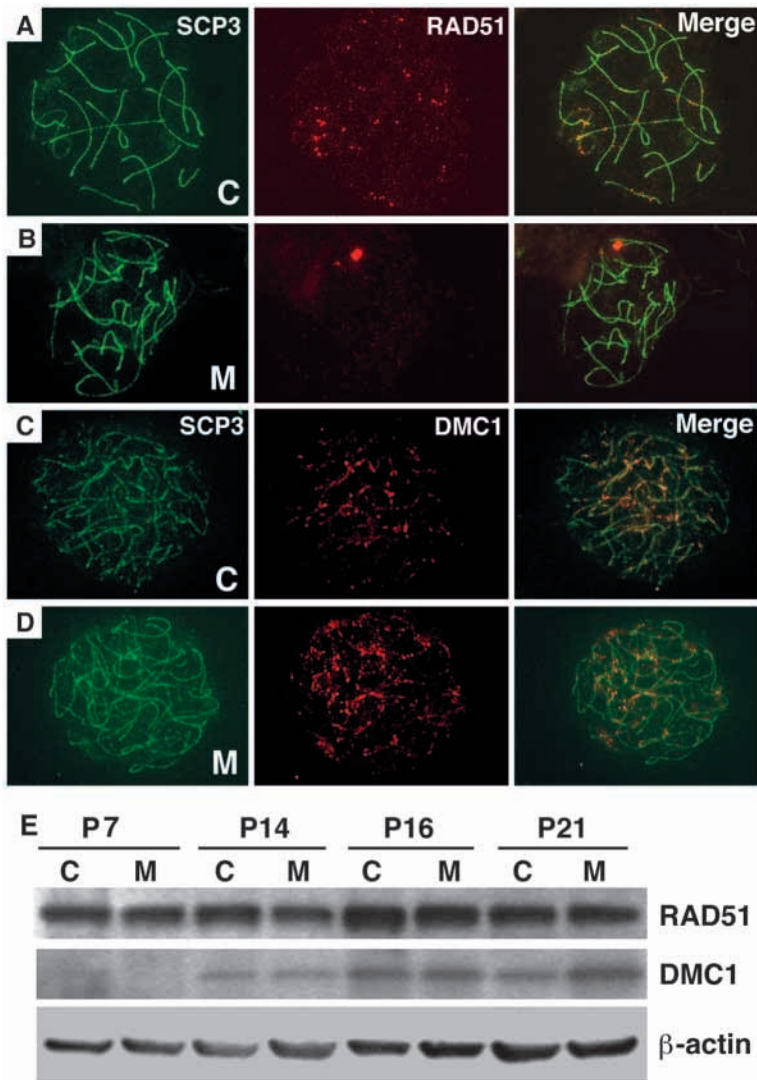


**Fig. 6.** Altered localization of Rad51, but not Dmc1, in *Brca1* mutant spermatocytes. Rad51 (A,B) and Dmc1 (C,D) double immunofluorescence localization of *p53*<sup>+/-</sup> and *Brca1*<sup>Δ11/Δ11</sup>*p53*<sup>+/-</sup> primary spermatocytes chromosomes at the pachytene (A,B) and zygotene (C,D) stages. Three pairs of mutant and control mice at P16, P18 and P21 were examined. There were significant differences in Rad51 foci formation between *Brca1* mutant and control mice (compare A with B;  $P \leq 0.0001$ ). (E) Western blot analysis of Rad51 and Dmc1 expression in *p53*<sup>+/-</sup> (C) and *Brca1*<sup>Δ11/Δ11</sup>*p53*<sup>+/-</sup> (M) testes. Genotypes, ages and antibodies are indicated.

#### Abnormal localization of Rad51, but not Dmc1, in *Brca1* mutant mice

Rad51 and Dmc1 are homologs of *Escherichia coli* RecA. They bind to DSBs and are involved in meiotic recombination repair (Masson and West, 2001). Because BRCA1 colocalizes with RAD51 on meiotic chromosomes and DMC1 colocalizes with RAD51 (Masson and West, 2001; Scully et al., 1997), we tested whether *Brca1* mutation affected localization of these proteins. In control spermatocytes, Rad51 foci started to appear on the chromosomes of leptotene-stage spermatocytes (Fig. 6A,  $n=176$ ) and disappeared on chromosomes from mid-pachytene-stage spermatocytes (data

not shown). Analyses of 211 spermatocytes from three *Brca1* mutant mice demonstrated significantly diminished numbers of Rad51 foci on all chromosomes (Fig. 6B). Western blots were performed to see if the failure to detect Rad51 on chromosomes was caused by reduced Rad51 protein concentrations. This analysis revealed comparable levels of Rad51 in *Brca1* mutant and control animals (Fig. 6E), suggesting that the absence of full-length *Brca1* isoform affected the localization of Rad51 but not the abundance. There were no apparent differences in Dmc1 localization and concentration between *Brca1* mutant and control mice on chromosomes isolated from >300 spermatocytes (Fig. 6C-E).

#### The localization pattern of $\gamma$ H2AX is altered in spermatocytes from *Brca1* mutant mice

H2AX is a member of the mammalian histone H2A family (reviewed by Redon et al., 2002). It is phosphorylated and relocated to DSBs within minutes of irradiation, which is consistent with a crucial role for this gene in DSB repair (Paull et al., 2000). H2AX-deficient mice display defective spermatogenesis and diminished numbers of *Brca1* chromosomal foci (Celeste et al., 2002). To determine if *Brca1* mutation alters H2AX phosphorylation and localization, chromosome spreads from P18, P21 and P28 testes of *Brca1* mutant ( $n=6$ ) and control ( $n=6$ ) mice were prepared and subjected to double staining with an antibody to SCP3 and an antibody specific for phosphorylated H2AX ( $\gamma$ H2AX). In control mice, we observed changes in  $\gamma$ H2AX staining at different stages of spermatogenesis. It appeared first as diffused staining in leptotene-stage spermatocytes (Fig. 7A) but evolved into distinctly stained foci on chromosomes from late leptotene and early zygotene-stage spermatocytes (Fig. 7B). Beginning at the late zygotene stage, staining was restricted to the sex (XY) body and became gradually brighter and more condensed (arrow, Fig. 7C) until  $\gamma$ H2AX localization was restricted to the sex body in almost all the cells examined (98%, 288 out of 304) throughout the pachytene stage (Fig. 7D). In *Brca1* mutant mice, the pattern of  $\gamma$ H2AX localization was similar to control mice at the leptotene and early zygotene stages (Fig. 7F,G). However, at the late zygotene and early pachytene stages, >90% (388 out of 427) of spermatocytes failed to show localization of  $\gamma$ H2AX to the XY body. Instead, it remained as multiple distinct foci (Fig. 7H,I). The intensity of staining in the 10% of cells that demonstrated  $\gamma$ H2AX localization in the XY body was decreased significantly (data not shown). The differences in the percentages of spermatocytes that showed  $\gamma$ H2AX staining in the presence and absence of *Brca1* mutation was highly significant ( $P \leq 0.0001$ ). This indicates that the localization pattern of  $\gamma$ H2AX was disrupted by *Brca1* mutation, similar to the disruptions of the Mlh1 and Rad51 patterns of localization.

Next we investigated possible reasons for the prolonged



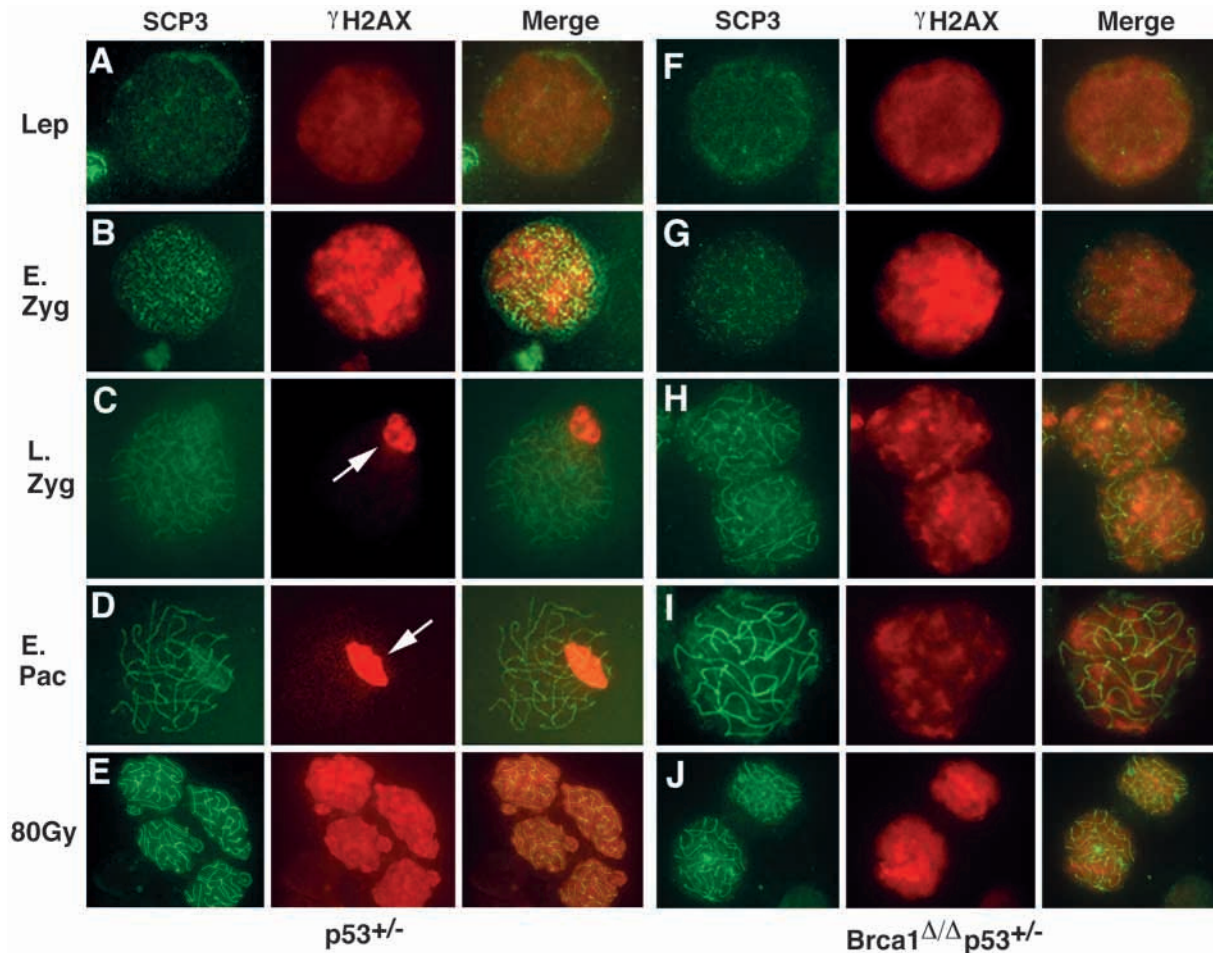


**Fig. 7.** Absence of the *Brca1* full-length isoform disrupted  $\gamma$ H2AX localization. Scp3 and  $\gamma$ H2AX double immunofluorescence localization of control and mutant spermatocytes. (A–D, F–I) Localization of  $\gamma$ H2AX in unirradiated testes. Localization is similar at the leptotene (Lep) and early zygotene (E. Zyg) stages in control and mutant spermatocytes. Starting from the late zygotene (L. Zyg) stage,  $\gamma$ H2AX localizes to the XY body in wild-type spermatocytes (arrows, C, D). However, in 90% of spermatocytes from *Brca1* mutant mice,  $\gamma$ H2AX fails to localize to the XY body and remains as multiple foci at the late zygotene stage (H) and early pachytene (E. Pac) stage (I). (E, J) Localization of  $\gamma$ H2AX in early pachytene stage spermatocytes 10 minutes after 80 Gy irradiation. The XY body cannot be detected.

presence of  $\gamma$ H2AX foci on the chromosomes and the absence of  $\gamma$ H2AX in the XY body. Because  $\gamma$ H2AX detects and binds to DSBs (Mahadevaiah et al., 2001), we suspected that the prolonged presence of  $\gamma$ H2AX foci in mutant cells could be caused by the accumulation of unrepaired DSBs. We further hypothesized that if sufficient DNA damage could be caused in control mice, they might exhibit defects similar to those observed in *Brca1* mutant mice. To test this, we irradiated control and *Brca1* mutant mice with 80 Gy of  $\gamma$ -irradiation to introduce acute, extensive DNA damage, and examined the formation of  $\gamma$ H2AX foci at various time points post irradiation. Spermatocytes were isolated from the irradiated mice at 10 minutes, 30 minutes, 2 hours and 4 hours following irradiation. All irradiated *p53*<sup>+/-</sup> spermatocytes demonstrated prolonged  $\gamma$ H2AX foci formation without XY body staining, similar to that found in the spermatocytes from unirradiated *Brca1* mutant mice (Fig. 7D). There were no differences in the numbers of  $\gamma$ H2AX foci in spermatocytes from irradiated *Brca1* mutant mice compared to those from irradiated control mice (Fig. 7H).

#### Steady-state RNA levels of RuvB-like DNA helicase, XPB, p62 and TFIID are reduced in *Brca1* mutant spermatocytes

Unwinding of parental DNA strands is a prerequisite for DNA replication, repair and recombination. The unwinding of duplex DNA is catalyzed by DNA helicases, which destabilize the hydrogen bonds between complementary double strands of DNA (Kanemaki et al., 1999). The absence of crossing-over in *Brca1* <sup>$\Delta$ 11/ $\Delta$ 11</sup>*p53*<sup>+/-</sup> mutant spermatocytes prompted us to measure the expression of genes that encode proteins with DNA helicase, branch migration and basic transcription activity. RNA samples from P14, P16, P21 and P22 were prepared from *p53*<sup>+/-</sup> control and *Brca1* <sup>$\Delta$ 11/ $\Delta$ 11</sup>*p53*<sup>+/-</sup> mutant mice. An appropriately sized RT-PCR product for p47, which encodes a RuvB-like DNA helicase, was detected in testes from both control and *Brca1* mutant mice. In RNA isolated from control testicular tissue, the RNA encoding p47 began to increase at P16 and was maintained at high levels through P22 (Fig. 8A). By contrast, the concentration of p47 RNA did not increase in testicular tissue from *Brca1* mutant animals (Fig.



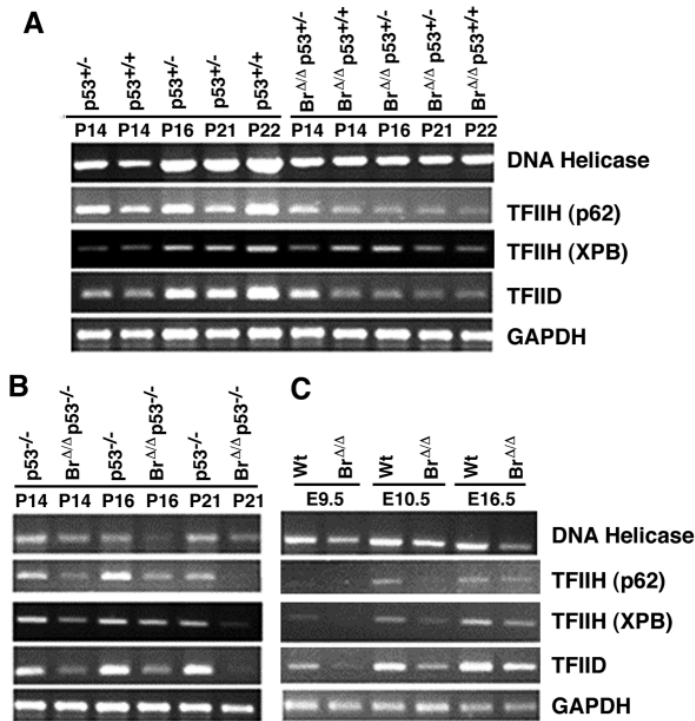


**Fig. 8.** Representative electrophoretic gels of RT-PCR products obtained using RNA isolated from mouse testes (A,B) and embryos (C). Genotypes, ages of the mice and primers used are indicated.

8A). The absence of an increase in p47 RNA during spermatogenesis in the absence of full-length Brca1 is consistent with the possibility that Brca1 could be a positive regulator of p47 expression during spermatogenesis.

Our data also revealed significant changes in the expression patterns of three additional genes that encode proteins that are involved in DSB repair. These are p62, a subunit of TFIIH, a basic transcription factor, XPB, a subunit of TFIIH with DNA-helicase activity, and TFIID, a basic transcription factor. As with p47, the concentrations of RNA encoding each of these proteins gradually increased from P14 to P22 in control animals, but not in spermatocytes of *Brca1* mutant mice (Fig. 8A). *Brca1* is known to regulate gene expression through both p53-dependent and p53-independent mechanisms. To determine if the changes in expression patterns of these genes were p53 dependent, patterns of gene expression were compared between *Brca1* mutant and wild type mice in a *p53*<sup>-/-</sup> background. Expression of all four genes was significantly lower in *Brca1*<sup>Δ11/Δ11</sup>*p53*<sup>-/-</sup> cells than in *Brca1*<sup>+/+</sup>*p53*<sup>-/-</sup> cells (Fig. 8B), indicating that the changes in expression patterns were independent of p53.

Because defective spermatogenesis began at P16 in *Brca1* mutant animals, one possible reason for the lack of increased expression of these genes in *Brca1* mutant mice could be the lack of spermatocytes at later ages (such as diplonema). If this were the case, lower expression levels would not necessarily be associated with absence of full-length Brca1. To test if lower expression levels directly correlated with absence of full-length Brca1, gene expression was examined in *Brca1* mutant embryos isolated from E9.5, E10.5 and E16.5 (Fig. 8C). These analyses demonstrated a direct correlation between the absence

of full-length Brca1 and lower expression levels of p47, p62, XPB and TFIID, which is consistent with the notion that Brca1 is a positive regulator of these genes.

## DISCUSSION

This study demonstrated an essential role for full-length Brca1 in spermatogenesis. Brca1 is required either directly or indirectly for repair of the double-stranded breaks that are introduced during the normal process of spermatocyte meiosis. By contrast, Brca1 does not appear to be required for oocyte meiosis. In *Brca1* mutant mice spermatogenesis did not advance beyond the pachytene stage of prophase during meiosis I and was accompanied by increased rates of apoptosis. Prophase of meiosis I involves in recombination between homologous chromosomes (reviewed by Cohen and Pollard, 2001; Roeder, 1997). This process requires extensive DNA damage-repair activity because defective meiosis can result from the individual loss-of-function of several different factors involved in DNA-damage repair (reviewed by Cohen and Pollard, 2001; Dasika et al., 1999; Tarsounas and Moens, 2001).

The majority of homologous chromosomes synapsed normally at the pachytene stage in spermatocytes isolated from *Brca1* mutant mice, indicating that *Brca1* is not required for this process. However, spermatocytes from *Brca1* mutant mice were arrested at the late pachytene stage and failed to enter the diplotene stage. This defect correlated with the absence of Mlh1 foci on the homologous chromosomes. Because Mlh1 foci localize to crossing-over sites on meiotic chromosomes and serve as a molecular marker for this event (Baker et al., 1996; Moens et al., 2002), it appears that full-length Brca1 is required for crossing-over. Crossing-over is a multi-step process that is initiated by a DSB in DNA, followed by exonucleolytic digestion, strand invasion, Holliday junction formation, branch migration and junction resolution, and, finally, heteroduplex DNA formation (reviewed by Cohen and Pollard, 2001; Roeder, 1997). It is possible that Brca1 is not required for the early steps of crossing-over because the phenotype of *Brca1*-deficient spermatocytes appeared at a later stage than those reported for SPO11-deficient (Romanienko and Camerini-Otero, 2000), ATM-deficient (Barlow et al., 1998), DMC1-deficient (Yoshida et al., 1998) and MSH4-deficient (Kneitz et al., 2000) spermatocytes.

Our data indicate a link between BRCA1 function and the proper localization of MLH1. Previous investigations revealed that MLH1, together with either MSH4/MSH5/PMS2 or MSH4/MSH5/MLH3, are involved in both mismatch repair and crossing-over (Cohen and Pollard, 2001). BRCA1 also displays an affinity for branched DNA structures and forms protein-DNA complexes cooperatively between multiple DNA strands without DNA sequence specificity (Paull et al., 2001). The results of the experiments presented here are consistent with the possibility that BRCA1 acts to recruit MLH1 to sites of recombination.

There are both similarities and differences between the phenotypes of *Brca1* and *Mlh1* deficient spermatocytes (Baker et al., 1996; Eaker et al., 2002). In both strains, the majority of homologous chromosomes undergo synapsis. A 10-100 fold reduction in chiasma formation is found in *Mlh1* mutant mice

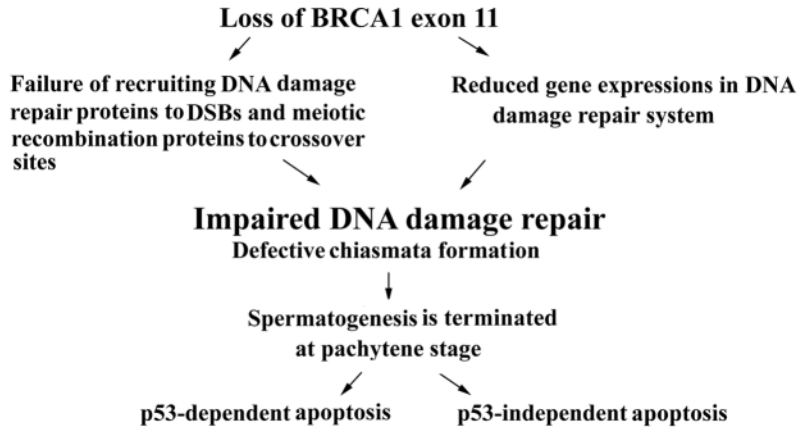


**Fig. 9.** Molecular events leading to defective spermatogenesis in *Brca1* full-length isoform-deficient mice. Two major functions of *Brca1* during spermatogenesis are emphasized: (1) recruiting DNA damage-repair proteins to damage sites; and (2) regulating RNA expression of genes involved in DNA-damage repair. Absence of the full-length isoform of *Brca1* results in impaired DNA-damage repair and leads to the termination of spermatocyte development at the pachytene stage by p53-dependent and p53-independent apoptosis.

whereas <1% of spermatocytes in *Brca1* mutant mice show any sign of chiasma formation and spermatocytes deficient in either protein have high rates of apoptosis. However, although *Brca1* mutant spermatocytes died at the end of the pachytene stage, the majority of *Mlh1* mutant spermatocytes die during metaphase (Eaker et al., 2002). It is interesting to note that the effect of *Brca1* mutation on formation of *Mlh1* foci is male specific because *Mlh1* foci are formed normally in oocytes.

In an attempt to further define the interaction between *BRCA1* and *MLH1*, we performed co-immunoprecipitation experiments between *BRCA1* and *MLH1* in human spermatocytes but could not detect any direct binding between these proteins (data not shown). Thus, the interaction between *BRCA1* and *MLH1* may be mediated indirectly through other proteins. Consistent with this, a mass-spectrometry study showed that *BRCA1* and other proteins, including *MSH2*, *MSH6*, *MLH1*, *ATM*, *BLM*, *RAD50*, *MRE11*, *NBS* and *RFC*, form a complex called *BRCA1*-associated genome-surveillance complex (*BASC*) (Wang et al., 2000) that is postulated to be involved in the recognition and repair of aberrant DNA structures. Wang et al. (2000) were able to demonstrate binding of *BRCA1* to *MSH2* and *MSH6*, both factors that bind directly to *MHL1*.

A candidate approach was used to study the localization and expression of several genes and gene products that are involved in various aspects of DNA-damage repair. We showed that distribution of *Rad51* on chromosomes was disrupted in testes from *Brca1* mutant mice. This finding is significant because *Rad51* is known to interact with *Brca1* either directly or indirectly after treatment with DNA-damaging reagents (Huber et al., 2001; Scully et al., 1997). Therefore, the abnormal distribution of *Rad51* in mutant chromosomes provides strong supporting evidence for the hypothesis that full-length *BRCA1* is required for the repair of DNA during meiosis in spermatocytes. Notably, the localization of *Dmcl1*, a closely related partner of *Rad51* (Masson and West, 2001; Tarsounas et al., 1999), was not altered, which indicates that loss of full-length *Brca1* disrupts the function of some but not all DNA damage-repair proteins.

Recent investigations have highlighted the interaction between  $\gamma$ H2AX and *BRCA1* and the importance of  $\gamma$ H2AX in DNA-damage repair. After using a laser beam to generate a DSB,  $\gamma$ H2AX becomes phosphorylated and moves to the site of the lesion within minutes (Paull et al., 2000). *BRCA1* moves to the same site approximately 45 minutes later. This suggests

that  $\gamma$ H2AX serves as a DNA damage sensor and that it is responsible for recruiting *BRCA1* to sites of DNA damage. In fact, *BRCA1* foci do not form on chromosomes from mice that lack H2AX, which results in increased genetic instability (Celeste et al., 2002).

At the late zygotene and early pachytene stages of normal spermatogenesis,  $\gamma$ H2AX relocates from sites of DSBs on chromosomes to the XY body. This did not occur in the absence of full-length *Brca1*. Instead,  $\gamma$ H2AX remained as multiple, distinct foci on chromosomes. Because  $\gamma$ H2AX binds to DNA prior to binding *Brca1* (Paull et al., 2000), it is likely that the binding of  $\gamma$ H2AX to DSBs is independent of *Brca1* and that the absence of full-length *Brca1* did not alter this process in spermatocytes. However, loss of full-length *Brca1* did block relocation of  $\gamma$ H2AX to the XY body. There are two possible explanations for this observation. First, recruitment of *Brca1* by  $\gamma$ H2AX may be essential for repairing DNA damage in spermatocytes. Therefore, in the absence of full-length *Brca1*, unrepaired DNA damage accumulates in the spermatocytes, which traps  $\gamma$ H2AX and prevents it from moving to the XY bodies. Experimental support for this possibility comes from the observation that the phenotypes of control spermatocytes that sustained extensive DNA damage from  $\gamma$ -irradiation and that of *Brca1* mutant spermatocytes were similar. Alternatively, *Brca1* could play a role that actively recruits  $\gamma$ H2AX to the XY body. The absence of *Brca1* consequently results in the failure of  $\gamma$ H2AX localization to the XY body. Recently, it has been proposed that *Brca1* is involved in X-chromosome inactivation (Ganesan et al., 2002). Future studies are needed to determine whether loss of localization of  $\gamma$ H2AX to the XY body in *Brca1* mutant spermatocytes affects X-inactivation.

Although *BRCA1* appears to regulate the expression of many genes that are involved in multiple biological processes (Chen et al., 1999; Deng and Brodie, 2000), only three of these genes are known to play a role in DNA-damage repair. These are *Gadd45* (a DNA damage-repair and response gene) (Harkin et al., 1999), *Ddb2* (which is defective in Xeroderma Pigmentosum group E cells and encodes the p48-damaged DNA-binding protein) (Takimoto et al., 2002) and *Xpc* (a gene encoding Xeroderma Pigmentosum group C complementing protein) (Hartman and Ford, 2002). All three genes are regulated by p53 and are involved in the nuclear excision-repair pathway (Hartman and Ford, 2002; MacLachlan et al., 2002; Takimoto et al., 2002). In this study, we found that loss of full-



length Brca1 correlated with decreased expression of several genes that encode proteins involved in the repair of DSBs, including RuvB-like DNA helicase, TFIIH (p62) and TFIIID. Additional investigations will determine if these genes are transcriptional targets of BRCA1 and if this regulation is direct or indirect.

The p53-dependent apoptotic pathway plays a dominant role in some but not all organs (reviewed by Burns and El-Deiry, 1999). We showed that spermatocyte apoptosis triggered by loss of full-length Brca1 was mediated by p53-dependent and p53-independent pathways. The most likely proximal trigger for both p53-dependent and p53-independent apoptosis in Brca1-deficient spermatocytes is the development of genetic instability. Thus, mutant spermatocytes that escaped the first wave of p53-dependent apoptosis survived slightly longer but still failed to progress into the diplotene stage. This suggests that activation of more than one apoptotic pathway ensures that spermatogenesis cannot be completed in the presence of significant genetic instability.

In summary, this study revealed that Brca1 plays an essential role in DNA-damage repair during spermatogenesis (Fig. 9). Brca1 functions through at least two different mechanisms, the recruitment of DNA damage-repair proteins to sites of DNA damage, and the regulation of the expression of DNA damage-repair genes. Examples of the first mechanism include the diminished numbers of Rad51 and Mlh1 foci on chromosomes in the absence of full-length Brca1. Examples of the second mechanism are the altered expression levels of RuvB-like DNA helicase, XPB, p62 and TFIIID in the absence of full-length Brca1. Thus, Brca1-deficient spermatocytes unavoidably accumulate unrepaired DNA damage that triggers both p53-dependent and p53-independent apoptosis, and failure of spermatogenesis.

We thank Drs L. P. K. Jones, M. Tilli, R. H. Wang, L. Cao, W. Qiao, and other members of Dr Furth's laboratory and Dr Deng's laboratory for their helpful discussions.

## REFERENCES

- Abbott, D. W., Thompson, M. E., Robinson-Benion, C., Tomlinson, G., Jensen, R. A. and Holt, J. T. (1999). BRCA1 expression restores radiation resistance in BRCA1-defective cancer cells through enhancement of transcription-coupled DNA repair. *J. Biol. Chem.* **274**, 18808-18812.
- Alberg, A. J. and Helzlsouer, K. J. (1997). Epidemiology, prevention, and early detection of breast cancer. *Curr. Opin. Oncol.* **9**, 505-511.
- Aprelikova, O., Pace, A. J., Fang, B., Koller, B. H. and Liu, E. T. (2001). BRCA1 is a selective co-activator of 14-3-3 sigma gene transcription in mouse embryonic stem cells. *J. Biol. Chem.* **276**, 25647-25650.
- Bachelier, R., Xu, X., Wang, X., Li, W., Naramura, M., Gu, H. and Deng, C. X. (2003). Normal lymphocyte development and thymic lymphoma formation in Brca1 exon 11-deficient mice. *Oncogene* (in press).
- Baker, S. M., Plug, A. W., Prolla, T. A., Bronner, C. E., Harris, A. C., Yao, X., Christie, D. M., Monell, C., Arnheim, N., Bradley, A. et al. (1996). Involvement of mouse Mlh1 in DNA mismatch repair and meiotic crossing over. *Nat. Genet.* **13**, 336-342.
- Baldeyron, C., Jacquemin, E., Smith, J., Jacquemont, C., De Oliveira, I., Gad, S., Feunteun, J., Stoppa-Lyonnet, D. and Papadopoulou, D. (2002). A single mutated BRCA1 allele leads to impaired fidelity of double strand break end-joining. *Oncogene* **21**, 1401-1410.
- Barlow, C., Liyanage, M., Moens, P. B., Tarsounas, M., Nagashima, K., Brown, K., Rottinghaus, S., Jackson, S. P., Tagle, D., Ried, T. et al. (1998). Atm deficiency results in severe meiotic disruption as early as leptotema of prophase I. *Development* **125**, 4007-4017.
- Brody, L. C. and Biesecker, B. B. (1998). Breast cancer susceptibility genes. BRCA1 and BRCA2. *Medicine (Baltimore)* **77**, 208-226.
- Burns, T. F. and El-Deiry, W. S. (1999). The p53 pathway and apoptosis. *J. Cell. Physiol.* **181**, 231-239.
- Cao, L., Li, W., Kim, S., Brodie, B. G. and Deng, C. X. (2003). Senescence, ageing and malignant transformation mediated by p53 in mice lacking Brca1 exon 11 isoform. *Genes Dev.* **17**, 201-213.
- Celeste, A., Petersen, S., Romanienko, P. J., Fernandez-Capetillo, O., Chen, H. T., Sedelnikova, O. A., Reina-San-Martin, B., Coppola, V., Meffre, E., Difilippantonio, M. J. et al. (2002). Genomic instability in mice lacking histone H2AX. *Science* **296**, 922-927.
- Chen, Y., Lee, W. H. and Chew, H. K. (1999). Emerging roles of BRCA1 in transcriptional regulation and DNA repair. *J. Cell. Physiol.* **181**, 385-392.
- Cohen, P. E. and Pollard, J. W. (2001). Regulation of meiotic recombination and prophase I progression in mammals. *BioEssays* **23**, 996-1009.
- Cressman, V. L., Backlund, D. C., Avrutskaya, A. V., Leadon, S. A., Godfrey, V. and Koller, B. H. (1999). Growth retardation, DNA repair defects, and lack of spermatogenesis in BRCA1-deficient mice. *Mol. Cell. Biol.* **19**, 7061-7075.
- Dasika, G. K., Lin, S. C., Zhao, S., Sung, P., Tomkinson, A. and Lee, E. Y. (1999). DNA damage-induced cell cycle checkpoints and DNA strand break repair in development and tumorigenesis. *Oncogene* **18**, 7883-7899.
- Deng, C. X. (2001). Tumorigenesis as a consequence of genetic instability in Brca1 mutant mice. *Mutat. Res.* **477**, 183-189.
- Deng, C. X. and Brodie, S. G. (2000). Roles of BRCA1 and its interacting proteins. *BioEssays* **22**, 728-737.
- Dobson, M. J., Pearlman, R. E., Karaskakis, A., Spyropoulos, B. and Moens, P. B. (1994). Synaptonemal complex proteins: occurrence, epitope mapping and chromosome disjunction. *J. Cell Sci.* **107**, 2749-2760.
- Eaker, S., Cobb, J., Pyle, A. and Handel, M. A. (2002). Meiotic prophase abnormalities and metaphase cell death in MLH1-deficient mouse spermatocytes: insights into regulation of spermatogenic progress. *Dev. Biol.* **249**, 85-95.
- Enders, G. C. and May, J. J., 2nd (1994). Developmentally regulated expression of a mouse germ cell nuclear antigen examined from embryonic day 11 to adult in male and female mice. *Dev. Biol.* **163**, 331-340.
- Ganesan, S., Silver, D. P., Greenberg, R. A., Avni, D., Drapkin, R., Miron, A., Mok, S. C., Randrianarison, V., Brodie, S., Salstrom, J. et al. (2002). BRCA1 Supports XIST RNA Concentration on the Inactive X Chromosome. *Cell* **111**, 393-405.
- Gowen, L. C., Avrutskaya, A. V., Latour, A. M., Koller, B. H. and Leadon, S. A. (1998). BRCA1 required for transcription-coupled repair of oxidative DNA damage. *Science* **281**, 1009-1012.
- Gowen, L. C., Johnson, B. L., Latour, A. M., Sulik, K. K. and Koller, B. H. (1996). Brca1 deficiency results in early embryonic lethality characterized by neuroepithelial abnormalities. *Nat. Genet.* **12**, 191-194.
- Hakem, R., de la Pompa, J. L., Sirard, C., Mo, R., Woo, M., Hakem, A., Wakeham, A., Potter, J., Reitmaier, A., Billia, F. et al. (1996). The tumor suppressor gene Brca1 is required for embryonic cellular proliferation in the mouse. *Cell* **85**, 1009-1023.
- Harkin, D. P., Bean, J. M., Miklos, D., Song, Y. H., Truong, V. B., Englert, C., Christians, F. C., Ellisen, L. W., Maheswaran, S., Oliner, J. D. et al. (1999). Induction of GADD45 and JNK/SAPK-dependent apoptosis following inducible expression of BRCA1. *Cell* **97**, 575-586.
- Hartman, A. R. and Ford, J. M. (2002). BRCA1 induces DNA damage recognition factors and enhances nucleotide excision repair. *Nat. Genet.* **32**, 180-184.
- Hohenstein, P., Kielman, M. F., Breukel, C., Bennett, L. M., Wiseman, R., Krimpenfort, P., Cornelisse, C., van Ommen, G. J., Devilee, P. and Fodde, R. (2001). A targeted mouse Brca1 mutation removing the last BRCT repeat results in apoptosis and embryonic lethality at the headfold stage. *Oncogene* **20**, 2544-2550.
- Huber, L. J., Yang, T. W., Sarkisian, C. J., Master, S. R., Deng, C. X. and Chodosh, L. A. (2001). Impaired DNA damage response in cells expressing an exon 11-deleted murine Brca1 variant that localizes to nuclear foci. *Mol. Cell. Biol.* **21**, 4005-4015.
- Kanemaki, M., Kurokawa, Y., Matsu-ura, T., Makino, Y., Masani, A., Okazaki, K., Morishita, T. and Tamura, T. A. (1999). TIP49b, a new RuvB-like DNA helicase, is included in a complex together with another RuvB-like DNA helicase, TIP49a. *J. Biol. Chem.* **274**, 22437-22444.
- Kneitz, B., Cohen, P. E., Avdievich, E., Zhu, L., Kane, M. F., Hou, H., Jr, Kolodner, R. D., Kucherlapati, R., Pollard, J. W. and Edelman, W. (2000). MutS homolog 4 localization to meiotic chromosomes is required

- for chromosome pairing during meiosis in male and female mice. *Genes Dev.* **14**, 1085-1097.
- Lane, T. F., Deng, C., Elson, A., Lyu, M. S., Kozak, C. A. and Leder, P.** (1995). Expression of Brca1 is associated with terminal differentiation of ectodermally and mesodermally derived tissues in mice. *Genes Dev.* **9**, 2712-2722.
- Liu, C. Y., Flesken-Nikitin, A., Li, S., Zeng, Y. and Lee, W. H.** (1996). Inactivation of the mouse Brca1 gene leads to failure in the morphogenesis of the egg cylinder in early postimplantation development. *Genes Dev.* **10**, 1835-1843.
- Ludwig, T., Chapman, D. L., Papaioannou, V. E. and Efstratiadis, A.** (1997). Targeted mutations of breast cancer susceptibility gene homologs in mice: lethal phenotypes of Brca1, Brca2, Brca1/Brca2, Brca1/p53, and Brca2/p53 nullizygous embryos. *Genes Dev.* **11**, 1226-1241.
- Ludwig, T., Fisher, P., Ganesan, S. and Efstratiadis, A.** (2001). Tumorigenesis in mice carrying a truncating Brca1 mutation. *Genes Dev.* **15**, 1188-1193.
- MacLachlan, T. K., Takimoto, R. and El-Deiry, W. S.** (2002). BRCA1 directs a selective p53-dependent transcriptional response towards growth arrest and DNA repair targets. *Mol. Cell Biol.* **22**, 4280-4292.
- Mahadevaiah, S. K., Turner, J. M., Baudat, F., Rogakou, E. P., de Boer, P., Blanco-Rodriguez, J., Jasin, M., Keeney, S., Bonner, W. M. and Burgoyne, P. S.** (2001). Recombinational DNA double-strand breaks in mice precede synapsis. *Nat. Genet.* **27**, 271-276.
- Masson, J. Y. and West, S. C.** (2001). The Rad51 and Dmc1 recombinases: a non-identical twin relationship. *Trends Biochem. Sci.* **26**, 131-136.
- Miki, Y., Swensen, J., Shattuck-Eidens, D., Futreal, P. A., Harshman, K., Tavtigian, S., Liu, Q., Cochran, C., Bennett, L. M., Ding, W. et al.** (1994). A strong candidate for the breast and ovarian cancer susceptibility gene BRCA1. *Science* **266**, 66-71.
- Moens, P. B., Kolas, N. K., Tarsounas, M., Marcon, E., Cohen, P. E. and Spyropoulos, B.** (2002). The time course and chromosomal localization of recombination-related proteins at meiosis in the mouse are compatible with models that can resolve the early DNA-DNA interactions without reciprocal recombination. *J. Cell Sci.* **115**, 1611-1622.
- Moynahan, M. E., Chiu, J. W., Koller, B. H. and Jasin, M.** (1999). Brca1 controls homology-directed DNA repair. *Mol. Cell* **4**, 511-518.
- Moynahan, M. E., Cui, T. Y. and Jasin, M.** (2001). Homology-directed DNA repair, mitomycin-c resistance, and chromosome stability is restored with correction of a Brca1 mutation. *Cancer Res.* **61**, 4842-4850.
- Paterson, J. W.** (1998). BRCA1: a review of structure and putative functions. *Dis. Markers* **13**, 261-274.
- Paull, T. T., Cortez, D., Bowers, B., Elledge, S. J. and Gellert, M.** (2001). From the cover: direct DNA binding by Brca1. *Proc. Natl. Acad. Sci. USA* **98**, 6086-6091.
- Paull, T. T., Rogakou, E. P., Yamazaki, V., Kirchgessner, C. U., Gellert, M. and Bonner, W. M.** (2000). A critical role for histone H2AX in recruitment of repair factors to nuclear foci after DNA damage. *Curr. Biol.* **10**, 886-895.
- Redon, C., Pilch, D., Rogakou, E., Sedelnikova, O., Newrock, K. and Bonner, W.** (2002). Histone H2A variants H2AX and H2AZ. *Curr. Opin. Genet. Dev.* **12**, 162-169.
- Roeder, G. S.** (1997). Meiotic chromosomes: it takes two to tango. *Genes Dev.* **11**, 2600-2621.
- Romanienko, P. J. and Camerini-Otero, R. D.** (2000). The mouse Spo11 gene is required for meiotic chromosome synapsis. *Mol. Cell* **6**, 975-987.
- Scully, R., Chen, J., Plug, A., Xiao, Y., Weaver, D., Feunteun, J., Ashley, T. and Livingston, D. M.** (1997). Association of BRCA1 with Rad51 in mitotic and meiotic cells. *Cell* **88**, 265-275.
- Shen, S. X., Weaver, Z., Xu, X., Li, C., Weinstein, M., Chen, L., Guan, X. Y., Ried, T. and Deng, C. X.** (1998). A targeted disruption of the murine Brca1 gene causes gamma-irradiation hypersensitivity and genetic instability. *Oncogene* **17**, 3115-3124.
- Snouwaert, J. N., Gowen, L. C., Latour, A. M., Mohn, A. R., Xiao, A., DiBiase, L. and Koller, B. H.** (1999). BRCA1 deficient embryonic stem cells display a decreased homologous recombination frequency and an increased frequency of non-homologous recombination that is corrected by expression of a brca1 transgene. *Oncogene* **18**, 7900-7907.
- Takimoto, R., MacLachlan, T. K., Dicker, D. T., Niitsu, Y., Mori, T. and el-Deiry, W. S.** (2002). BRCA1 transcriptionally regulates damaged DNA binding protein (DDB2) in the DNA repair response following UV-irradiation. *Cancer Biol. Ther.* **1**, 177-186.
- Tarsounas, M., Morita, T., Pearlman, R. E. and Moens, P. B.** (1999). RAD51 and DMC1 form mixed complexes associated with mouse meiotic chromosome cores and synaptonemal complexes. *J. Cell Biol.* **147**, 207-220.
- Tarsounas, M. and Moens, P. B.** (2001). Checkpoint and DNA-repair proteins are associated with the cores of mammalian meiotic chromosomes. *Curr. Top. Dev. Biol.* **51**, 109-134.
- Wang, Y., Cortez, D., Yazdi, P., Neff, N., Elledge, S. J. and Qin, J.** (2000). BASC, a super complex of BRCA1-associated proteins involved in the recognition and repair of aberrant DNA structures. *Genes Dev.* **14**, 927-939.
- Xu, X., Qiao, W., Linke, S. P., Cao, L., Li, W. M., Furth, P. A., Harris, C. C. and Deng, C. X.** (2001). Genetic interactions between tumor suppressors Brca1 and p53 in apoptosis, cell cycle and tumorigenesis. *Nat. Genet.* **28**, 266-271.
- Xu, X., Weaver, Z., Linke, S. P., Li, C., Gotay, J., Wang, X. W., Harris, C. C., Ried, T. and Deng, C. X.** (1999a). Centrosome amplification and a defective G2-M cell cycle checkpoint induce genetic instability in BRCA1 exon 11 isoform-deficient cells. *Mol. Cell* **3**, 389-395.
- Xu, X., Wagner, K. U., Larson, D., Weaver, Z., Li, C., Ried, T., Hennighausen, L., Wynshaw-Boris, A. and Deng, C. X.** (1999b). Conditional mutation of Brca1 in mammary epithelial cells results in blunted ductal morphogenesis and tumour formation. *Nat. Genet.* **22**, 37-43.
- Yoshida, K., Kondoh, G., Matsuda, Y., Habu, T., Nishimune, Y. and Morita, T.** (1998). The mouse RecA-like gene Dmc1 is required for homologous chromosome synapsis during meiosis. *Mol. Cell* **1**, 707-718.
- Zabludoff, S. D., Wright, W. W., Harshman, K. and Wold, B. J.** (1996). BRCA1 mRNA is expressed highly during meiosis and spermiogenesis but not during mitosis of male germ cells. *Oncogene* **13**, 649-653.
- Zhong, Q., Boyer, T. G., Chen, P. L. and Lee, W. H.** (2002a). Deficient nonhomologous end-joining activity in cell-free extracts from Brca1-null fibroblasts. *Cancer Res.* **62**, 3966-3970.
- Zhong, Q., Chen, C. F., Chen, P. L. and Lee, W. H.** (2002b). BRCA1 facilitates microhomology-mediated end joining of DNA double strand breaks. *J. Biol. Chem.* **277**, 28641-28647.
- Zickler, D. and Kleckner, N.** (1999). Meiotic chromosomes: integrating structure and function. *Annu. Rev. Genet.* **33**, 603-754.